Potassium Currents in Presynaptic Hair Cells of *Hermissenda*

Ebenezer N. Yamoah
Department of Physiology, Johns Hopkins School of Medicine, Baltimore, Maryland 21205 and Marine Biological Laboratory, Woods Hole, Massachusetts 02543

ABSTRACT Apart from their primary function as balance sensors, *Hermissenda* hair cells are presynaptic neurons involved in the Ca^{2+}-dependent neuronal plasticity in postsynaptic B photoreceptors that accompanies classical conditioning. With a view to beginning to understand presynaptic mechanisms of plasticity in the vestibulo-visual system, a locus for conditioning-induced neuronal plasticity, outward currents that may govern the excitability of hair cells were recorded by means of a whole-cell patch-clamp technique. Three K^+ currents were characterized: a 4-aminopyridine-sensitive transient outward K^+ current (I_A), a tetraethyl ammonium–sensitive delayed rectifier K^+ current ($I_{K,V}$), and a Ca^{2+}-activated K^+ current ($I_{K,Ca}$). I_A activates and decays rapidly; the steady-state activation and inactivation curves of the current reveal a window current close to the apparent resting voltage of the hair cells, suggesting that the current is partially activated at rest. By modulating firing frequency and perhaps damping membrane oscillations, I_A may regulate synaptic release at baseline. In contrast, $I_{K,V}$ and $I_{K,Ca}$ have slow onset and exhibit little or no inactivation. These two K^+ currents may determine the duration of the repolarization phase of hair-cell action potentials and hence synaptic release via Ca^{2+} influx through voltage-gated Ca^{2+} channels. In addition, $I_{K,Ca}$ may be responsible for the afterhyperpolarization of hair cell membrane voltage following prolonged stimulation.

INTRODUCTION

Alteration of presynaptic activity may be an essential component in mechanisms of long-term neuronal plasticity (Bekkers and Stevens, 1990). Previous studies of hippocampal neurons and sensory neurons in *Aplysia* have shown that the induction, and perhaps the maintenance, of long-term plasticity may require simultaneous stimulation of both presynaptic and postsynaptic neurons (Abrams and Kandel, 1988; Bekkers and Stevens, 1990; Chavez-Noriega and Stevens, 1994). Similarly, in the vestibulo-visual system of *Hermissenda*, a locus for associative conditioning-induced neuronal plasticity, contiguous stimulation of presynaptic hair cells and postsynaptic photoreceptors are required for long-term membrane biophysical alterations in the photoreceptors (Crow, 1988; Matzel and Rogers, 1993). Remarkably, there is little direct information on the mechanism(s) by which input from the hair cells contributes to long-term membrane modification of the photoreceptors (Alkon et al., 1992; Rogers et al., 1994). Ionic currents in the hair cells have not been characterized, and the possible role of the hair cells in conditioning-induced plasticity has not been examined. However, recent evidence suggests that paired release of γ-aminobutyric acid (GABA) from hair cells to synaptic terminals of the photoreceptors induce changes similar to that reported for conditioned animals (Matzel and Alkon, 1991). GABA decreases membrane input resistance (Alkon et al., 1992) and baclofen, a $GABA_B$ receptor agonist, increases K^+ conductance in the type-B photoreceptors (Rogers et al., 1994; Matzel et al., 1995). Furthermore, GABA enhances Ca^{2+} currents at low concentrations in the photoreceptors (Yamoah and Crow, 1996), which is consistent with the observation that GABA increases intracellular Ca^{2+} concentration at the postsynaptic terminals of the photoreceptors (Alkon et al., 1992). Stimulation of hair cells may results in the release of serotonin at the synaptic terminals of the photoreceptors, perhaps through interneurons (Land and Crow, 1985; Farley and Wu, 1987). Release of either GABA or serotonin depends on Ca^{2+} influx, which in turn depends on the excitability of the membrane properties of the hair cells. Thus, studies of the ionic conductances that govern membrane properties of hair cells are pertinent to the understanding of the presynaptic mechanisms of plasticity in *Hermissenda*.

Hair cells form part of the statocyst organ in mollusks. *Hermissenda* hair cells are spherical in shape with diameters of ~30–~40 μm and bear ~100 kinocilia and microvilli (Kuzirian et al., 1981), in contrast to vertebrate hair cells, which may have a single kinocilium and 50–100 stereocilia, depending on the species (Hudspeth and Jacobs, 1979). In both cases, however, the kinocilia transmit rather than directly transduce mechanical stimuli (Hudspeth and Jacobs, 1979; Stommel et al., 1980). In response to gravitational stimulus, *Hermissenda* hair cells interact physically with the statoconia to activate nonspecific cation channels (Alkon, 1975; DeFelice and Alkon, 1977; Stommel et al., 1980). Apart from the mechanosensitive current (Alkon and Bak, 1973), there is an array of voltage- and time-dependent ionic currents present within the plasma membrane of the soma and axons of hair cells that are responsible for generation of trains of spikes that are conducted to the brain for integration and response. Vertebrate hair cells, on the other hand,

Received for publication 15 May 1996 and in final form 7 October 1966.
Address reprint requests to Dr. Ebenezer N. Yamoah, Department of Physiology, Johns Hopkins School of Medicine, 725 North Wolfe Street, Baltimore, MD 21205. Tel: 410-614-3082; Fax: 410-955-0461; E-mail:eyamoah@welchlink.welch.jhu.edu.
© 1997 by the Biophysical Society
0006-3495/97/01/193/11 $2.00

normally do not elicit action potentials. By isolating the statocyst organ and carefully removing the capsule surrounding the organ, one can study individual hair cells by using the whole-cell voltage-clamp technique. Here, I present the kinetic and pharmacologic description of the voltage-, time-, and Ca^{2+}-dependent outward K^+ currents in presynaptic hair cells of *Hermissenda*. Three distinct K^+ currents are expressed in the soma of the hair cells: a fast and rapidly inactivating 4-aminopyridine (4-AP-) sensitive A-type current (I_A), a tetraethyl ammonium– (TEA-) sensitive delayed rectifier current, which exhibits slow inactivation kinetics ($I_{K,V}$), and a TEA- and 4-AP-insensitive Ca^{2+}-dependent current ($I_{K,Ca}$). The three currents may play different roles in the excitability of the hair cells and thus contribute to the modulation of synaptic release.

MATERIALS AND METHODS

Isolation of statocyst and hair cells

Experiments were performed on both isolated hair cells and hair cells attached to axotomized statocyst of *Hermissenda* (Sea-Life Supply, Sand City, CA). The nervous systems were isolated and treated with an enzyme solution consisting of protease (1 mg/ml) and dispase (7 mg/ml) in artificial seawater at 4°C for 10–20 min. The nervous systems were then transferred to fresh enzyme solution at room temperature for 10–20 min. The statocysts were removed and transferred into a 35-mm sterile culture dish, which contained 1.5 ml (Ca^{2+}-free) 0.1 mM EGTA artificial seawater, and incubated at 4°C for 10–15 min to loosen the tight junctions between hair cells and supporting cells. The static nerve was removed, and individual hair cells were isolated with a suction pipette. Voltage-clamp experiments were performed on isolated hair cells and in hair cells attached to the axotomized statocyst. Current records were similar in both experimental conditions.

Chemicals and solutions

Chemicals were obtained from Sigma Chemical Co. (St. Louis, MO). Solutions used and their chemical compositions (in mM) were 1) artificial seawater: 420 NaCl, 10 KCl, 10 $CaCl_2$, 50 $MgCl_2$, 15 *N*-[2-hydroxyethyl]piperazine-*N*′-[2-ethanesulfonic acid] (HEPES), pH 7.8 (NaOH); 2) external solution for K^+-current recordings: 200 *N*-methyl-D-glucamine, 300 choline chloride, 10–70 KCl, 0–50 $CaCl_2$, 10–60 $MgSO_4$, 15 HEPES, pH 7.7 (KOH); 3) pipette solution for K^+-current recordings: 20 NaCl, 2 $MgSO_4$, 50 HEPES, 0.2–10 ethyleneglycol-bis-(β-amino-ethylether)*N*,*N*′-tetra-acetic acid (EGTA), 200–400 KCl, 250 NMG, 5 MgATP, 1 Na_2GTP, 10 reduced glutathione, pH 7.4 (HCl). Osmolarity of all solutions ranged between 960 and 1000 mosmol. Similar solutions have been used successfully in recording potassium currents in the photoreceptors of *Hermissenda* (Yamoah and Crow, 1995). Stock solutions of 50 mM 4-aminopyridine (4-AP) and 400 mM tetraethylammonium (TEA) were made and stored at −20°C. Aliquots of these solutions were diluted in the recording solution and superfused at a rate of 5 ml/min in a 0.5-ml experimental chamber.

Electophysiologic recording and data analysis

Experiments were performed at room temperature (21°C). The whole-cell patch-clamp method (Hamill et al., 1981) was used to record K^+ currents by use of an Axopatch 200A amplifier (Axon Instruments, Foster City, CA). Data were low-pass-Bessel filtered at a cutoff frequency of 5 kHz, digitized at a sampling frequency of 10 kHz with a Digidata interface (Axon Instruments), and stored in a personal computer. Experimental protocols were controlled by the computer with pClamp V. 5.7.1 software (Axon Instruments). Passive leakage and capacitive currents were subtracted by the p/-4 method. The sum of currents elicited by four hyperpolarizing pulses from the holding potential with an amplitude one-fourth of the test pulse was added to the test-pulse-induced current. The resistance in series (R_s) with the membrane resistance was assessed, and 40–60% was canceled electronically (pipette and series resistance, 1.5 ± 0.2 MΩ, N = 45 and 4.88 ± 1.51 MΩ, N = 32, respectively; mean ± SD). Cell capacitance (C_m) was 32 ± 9 pF, N = 29. Data were accepted for analysis according to the criteria described earlier (Yamoah and Crow, 1994). Liquid junction potential of 3–6 mV was measured, depending on the external and pipette solutions used for the experiments. Liquid junction potential was adjusted to determine the reversal potentials of the currents. Data were analyzed with the Clampfit routine of the pClamp program (Axon Instruments). Curve fits were performed by the least-squares method with Sigmaplot software (Jandel Scientific, San Rafael, CA) and Microcal Origin (Microcal Software Inc., Northampton, MA). Unless indicated, data are presented as mean ± SD. Dose response relationships were described by use of a logistic function:

$$\frac{A_1 - A_2}{1 + (X/X_0)^p} + A_2. \tag{1}$$

Here A_1 and A_2 are the initial and the final current ratios, respectively, X is the concentration of drug, X_0 is the half-blocking or activation concentration, and p is the Hill coefficient. The steady-state activation (m_∞) and inactivation (h_∞) properties of the currents in relation to voltage were described by the Boltzmann equations

$$m_\infty = \frac{1}{1 + \exp(V_{1/2} - V/K_m)}, \tag{2}$$

$$h_\infty = \frac{1}{1 + \exp(V - V_{1/2}/K_h)}, \tag{3}$$

where V is the membrane voltage, $V½$ denotes the half-activation or inactivation voltage, and K is the slope factor. The I_A current records were fitted to a modified form of the Hodgkin–Huxley equation to yield activation (τ_m) and inactivation (τ_h) time constants. Data records were fitted to

$$i(t) = \bar{i}\left[1 - \exp - \left(\frac{t-\delta}{\tau_m}\right)\right]^4 \cdot \left[\exp - \left(\frac{t-\delta}{\tau_{h1}}\right) + r \exp - \left(\frac{t-\delta}{\tau_{h2}}\right)\right], \tag{4}$$

where $\bar{i}$ refers to the maximum current; a time delay, δ, was included to allow for the slowing of the voltage-clamp steps owing to uncompensated series resistance; τ_m is the activation and τ_{h1} and τ_{h2} are the two phases of inactivation time constants; the parameter r refers to the relative contribution of the "fast" and "slow" phases of the inactivation time course.

The steady-state current can be described in terms of m_∞ and h_∞ as follows:

$$i = m_\infty^4 h_\infty \bar{g}(V_m - V_{rev}), \tag{5}$$

where $\bar{g}$ represents the maximum channel conductance; V_m, the membrane potential; and V_{rev}, the reversal potential. Equation 4 was modified to fit $I_{K,V}$. Here, the inactivation component of the equation was removed.

RESULTS

Isolation of three components of K^+ currents

Macroscopic K^+ currents were recorded in isolated hair cells and in hair cells attached to the axotomized statocyst. Inasmuch as electrical coupling between hair cells occurs at the axonal region distal to the soma (Detwiler and Alkon, 1973), removal of the static nerve was sufficient for ade-

quate voltage clamp. Na^+ and Ca^{2+} were removed by ionic substitution with choline. Ca^{2+} was added to the bath solution when the Ca^{2+}-dependent K^+ current was studied. Fig. 1 shows two components of outward currents recorded in Ca^{2+}-free media. Outward currents evoked from a holding potential of −80 mV show an early transient and a sustained component. Fig. 1 *A* illustrates a family of outward current traces elicited by use of voltage-clamp steps from −90 mV to 40 mV with 7-mV increments from a holding potential of −80 mV. The transient component was activated at step voltages positive to −55 mV, followed by a sustained component at step voltages positive to −25 mV. By use of a holding potential of −30 mV, the transient component of the outward current was inactivated, and a relatively slow onset current with slow inactivation kinetics became apparent (Fig. 1 *B*). Current–voltage relations of records obtained at holding potentials of −80 and −30 mV are shown in Fig. 1 *C*.

To characterize the different components of the outward currents evoked from hyperpolarizing potential of −80 mV to various levels of depolarization, 4-AP, TEA, and Ca^{2+} or combinations of these agents were applied to the external solution. Whereas 4-AP and TEA are known blockers of the transient outward and delayed rectifier currents, respectively (Hille, 1992; Norris et al., 1992; Choquet and Korn, 1992), Ca^{2+} has been shown to activate an outward K^+ current (Meech, 1974). Fig. 2*A* and *B* illustrates families of outward currents recorded in the absence and in the presence, respectively, of 5 mM 4-AP. Addition of 4-AP to the external solution rapidly resulted in the removal of the fast inactivation component of the current and a reduction in the amplitude of the whole-cell outward current. 4-AP strongly reduced the amplitude of the transient outward current but had only a small effect on the sustained current. The effects of 4-AP on the transient current were concentration dependent. Shown in Fig. 2 *E* is the dose-response curve of 4-AP for the transient current. Here, the transient current was evoked from a holding potential of −90 mV to 9 step potential −35 mV in Ca^{2+}-free external solution. The half-blocking concentration of 4-AP was 0.9 ± 0.3 mM (n = 7).

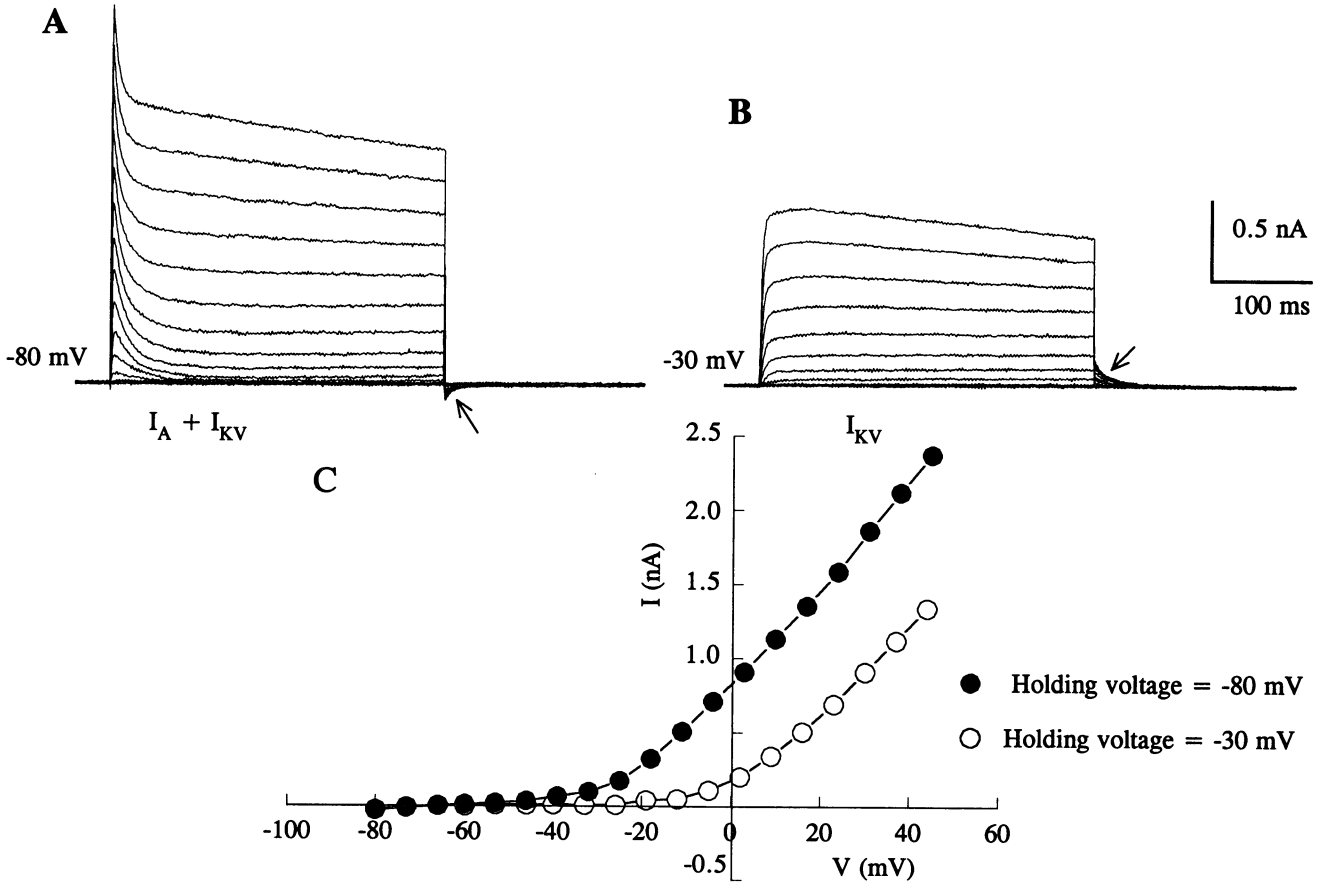

FIGURE 1 Characteristics of outward currents in isolated hair cells. *A*, Family of outward currents elicited from a holding potential (V_h) of −80 mV to step potentials (*Vn*) from −90 to 40 mV in 7-mV increments, illustrating the voltage dependence of the currents. The outward current had a rapid onset followed by a fast inactivating component and then a sustained component. At V_h of −80 mV the outward current had an inwardly directed tail current (*arrow*). *B*, At V_h of −30 mV the transient fast inactivating component of the current traces in *A* was suppressed. A delayed onset current with slow inactivation became apparent. In contrast to the traces generated from V_h of −80 mV, the tail currents at V_h of −30 mV were outward (*arrow*). *C*, Peak current–voltage relations of outward currents at V_h of −80 mV (●) and of −30 mV (○). The outward current began to activate at ~−55 mV from a holding potential of −80 mV.

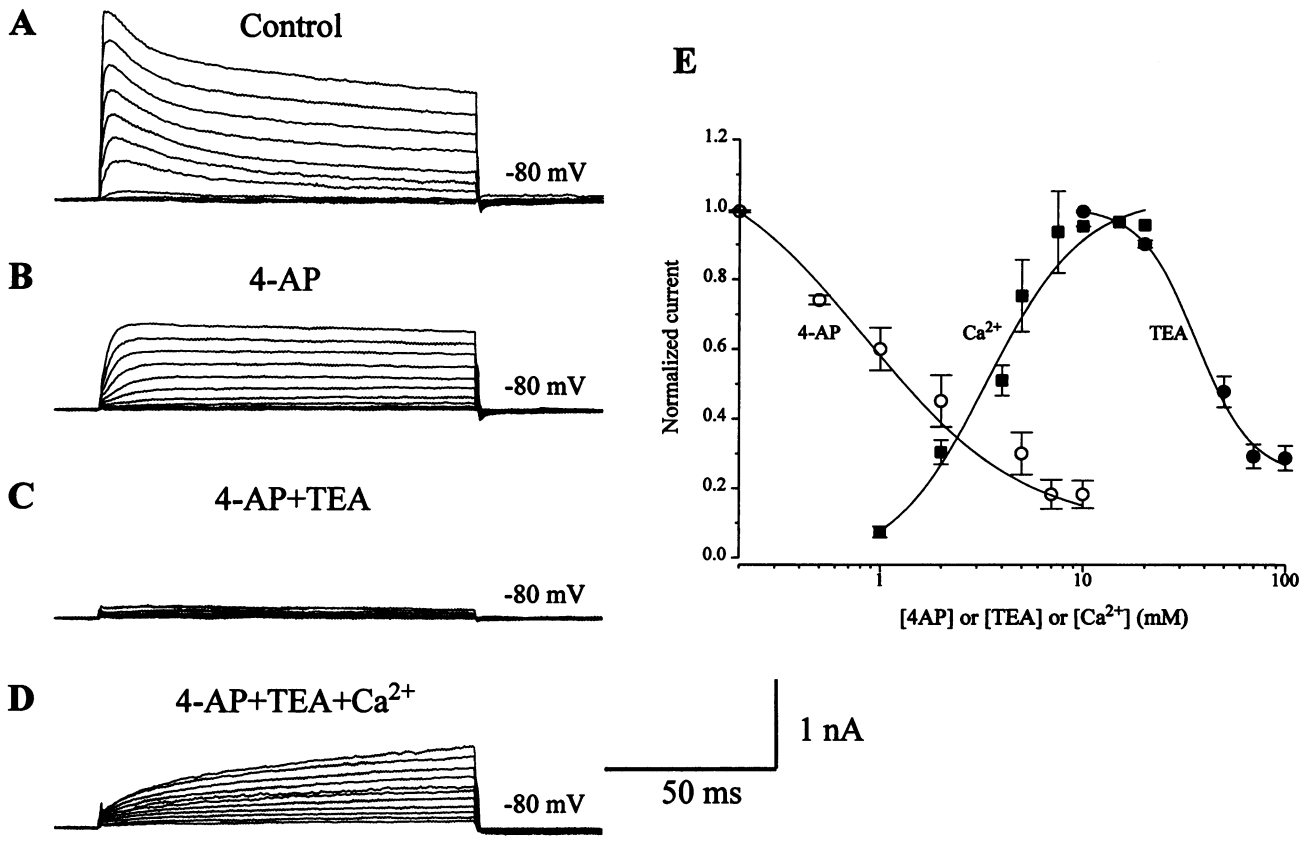

FIGURE 2 Determination of the different components of the outward currents. *A*, Current traces evoked from a hair cell from a holding potential of −80 mV and stepped to incremental depolarizing voltages of 8 mV. *B*, On application of 5 mM 4-AP, two effects were observed from the traces evoked under conditions similar to those for *A*. The current magnitude was reduced, and the inactivating component of the currents in *A* was abolished. *C*, The remaining current (4-AP-insensitive current) was abolished when the bath solution was superfused with 5 mM 4-AP and 90 mM TEA. *D*, As the $[Ca^{2+}]$ in the bath was increased, there emerged a third outward current. Shown are current traces evoked in the presence of 5 mM Ca^{2+}, 5 mM 4-AP, and 90 mM TEA. *E*, Concentration dependence of the different components of the outward currents on 4-AP, TEA, and Ca^{2+}. The transient current, I_A, was evoked from −90 to −35 mV, and the TEA-sensitive current, $I_{K,V}$, was elicited from −30 to 20 mV. Similar voltage steps were used to activate $I_{K,Ca}$; however, here the experiments were performed in the presence of 5 mM 4-AP and 100 mM TEA. The estimated half-blocking and -activating concentration of 4-AP was 0.9 ± 0.3 mM (n = 7), that of TEA was 36 ± 4 mM (n = 5), and that of Ca^{2+} was 3.4 ± 0.6 mM (n = 6).

The sustained outward current remaining after the application of 4-AP was substantially reduced on the addition of 90 mM TEA in the external solution (Fig. 2 *C*). Blocking of the sustained current by TEA was concentration dependent, and the half-blocking concentration of TEA as shown in the dose-response curve in Fig. 2 *E* was 36 ± 4 mM (n = 5). The residual current after applications of 4-AP and TEA was enhanced as the external $[Ca^{2+}]$ was increased from 0 to 5 mM (Fig. 2 *D*). The Ca^{2+}-dependent current had a delayed onset and exhibited no inactivation. The relationship between external Ca^{2+} and the outward current is shown in Fig. 2 *E*, and the estimated half-activation concentration of Ca^{2+} is 3.4 ± 0.6 mM (n = 6). These three components of the outward K^+ currents are studied in more detail below.

Reversal potential of the outward currents

To determine the ionic composition of the outward currents, I investigated the reversal potentials of the currents by assessing tail currents at various external K^+ concentrations. For control recording conditions (250 mM internal K^+ and 10 mM external K^+), tail currents were inward at potentials more negative to −77 mV but became outward at potentials more positive to −70 mV. An increase in external $[K^+]$ shifted the reversal potential to more positive potentials. Illustrated in Fig. 3 *A* are traces of the TEA-sensitive current ($I_{K,V}$) evoked from a holding potential of −40 mV by a 60-ms depolarizing step to 40 mV. The depolarization was followed by potential levels from 50 mV to −150 mV, and the amplitude of the tail current was then examined. The average reversal potential was −73 ± 2 mV (n = 7) for control solutions (Fig. 3 *B*). Fig. 3 *C* shows changes in E_{rev} as the bath $[K^+]$ was raised from 10 to 70 mM. The changes in E_{rev} roughly approximated that predicted by the Nernst equation. E_{rev} calculated for the transient current was −75 ± 5 mV (n = 5). In contrast, alteration of both the bath and the pipette $[Cl^-]$ was independent of the direction of the shifts in the reversal potential (not shown).

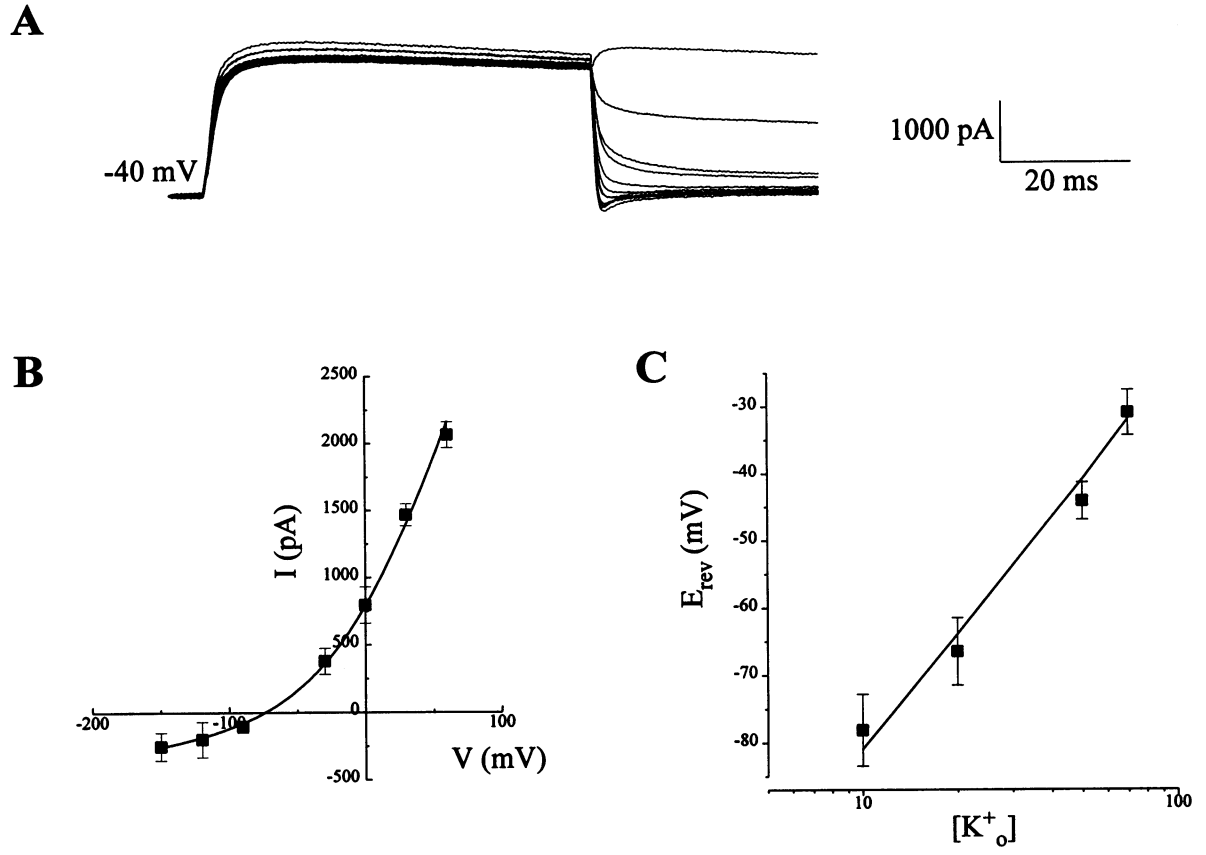

FIGURE 3 Reversal potential of the sustained component of outward current at different concentrations of external K^+. Cells were held at −40 mV, and outward currents were elicited for 60 ms to 40 mV. At the end of the test pulse the membrane potential was repolarized to different potentials in 20-mV increments (between −150 and 50 mV), and the tail currents were examined. The current traces from a single hair cell are illustrated in *A*, and the averaged instantaneous current–voltage relationship is shown in *B* (data collected from five cells). The current was recorded in 10 mM external K^+ and 250 mM pipette K^+. The continuous line represents fit to the Goldman–Hodgkin–Katz equation (Hille, 1992), with a calculated reversal potential (E_{rev}) of −73 mV. When the external K^+ concentration was varied from 10 to 70 mM and the pipette K^+ concentration (250 mM) was maintained, the reversal potential shifted from −78 ± 5 mV in 10 mM to −31 ± 3 in 70 mM (n = 5), as illustrated in *C*. The theoretical relationship between E_{rev}, as predicted by the Goldman–Hodgkin–Katz equation, and the changes in external $[K^+]$ is shown by a straight line. The observation justifies the conclusion that K^+ is the predominant charge carrier of the outward current.

Properties of the transient outward K^+ current

Because the transient outward current shares characteristic sensitivity toward 4-AP, the current will be denoted I_A in accordance with the established nomenclature (Hille, 1992). The half-maximal activation voltage and the slope factor of the steady-state activation curve were −31 ± 1 mV and 7.9 ± 0.4 mV (n = 9), respectively (Fig. 4 *A*). To prevent the possible complication of altered kinetics of the current by pharmacological blockers, inactivation of I_A was assessed in the absence of TEA. The steady-state inactivation was investigated by application of a 550 ms conditioning pulse to various potentials between −80 and 30 mV, followed by a test pulse to 0 mV (*inset*, Fig. 4 *A*). The steady-state current elicited at the test pulse was subtracted from the total current to generate the inactivation curve (Fig. 4 *A*). I_A was half-inactivated at −51 ± 0.8 mV, and the curve had a slope factor of 6.0 ± 0.3 mV (n = 7). The steady-state activation and inactivation curves overlapped, with a window conductance ranging from −50 to −30 mV with a maximum at −42 mV (Fig. 4 *A*). The window conductance persisted but was reduced when the activation curve (m_∞) was shifted by an m_∞^4 function, a best fit for the activation kinetics (Fig. 4 *B*).

To determine the profile of the 4-AP-sensitive outward current, I subtracted current traces generated in the presence of 4-AP from the control traces. The resulting current traces in Fig. 4 *B* show outward currents with rapid onset and decay. The time course of activation and inactivation at various step potentials was assessed by the modified Hodgkin–Huxley formalism as outlined in Eq. 4. Here, the fits were performed on difference current traces as illustrated in Fig. 4 *B*. Figure 4 *C* shows the activation (τ_m) and inactivation (τ_{h1}) time constants, with τ_m ranging from 2.3 to 10 ms and τ_{h1} ranging from 15 to 45 ms.

In another series of experiments, the time-dependent inactivation of I_A at various voltages was determined by use

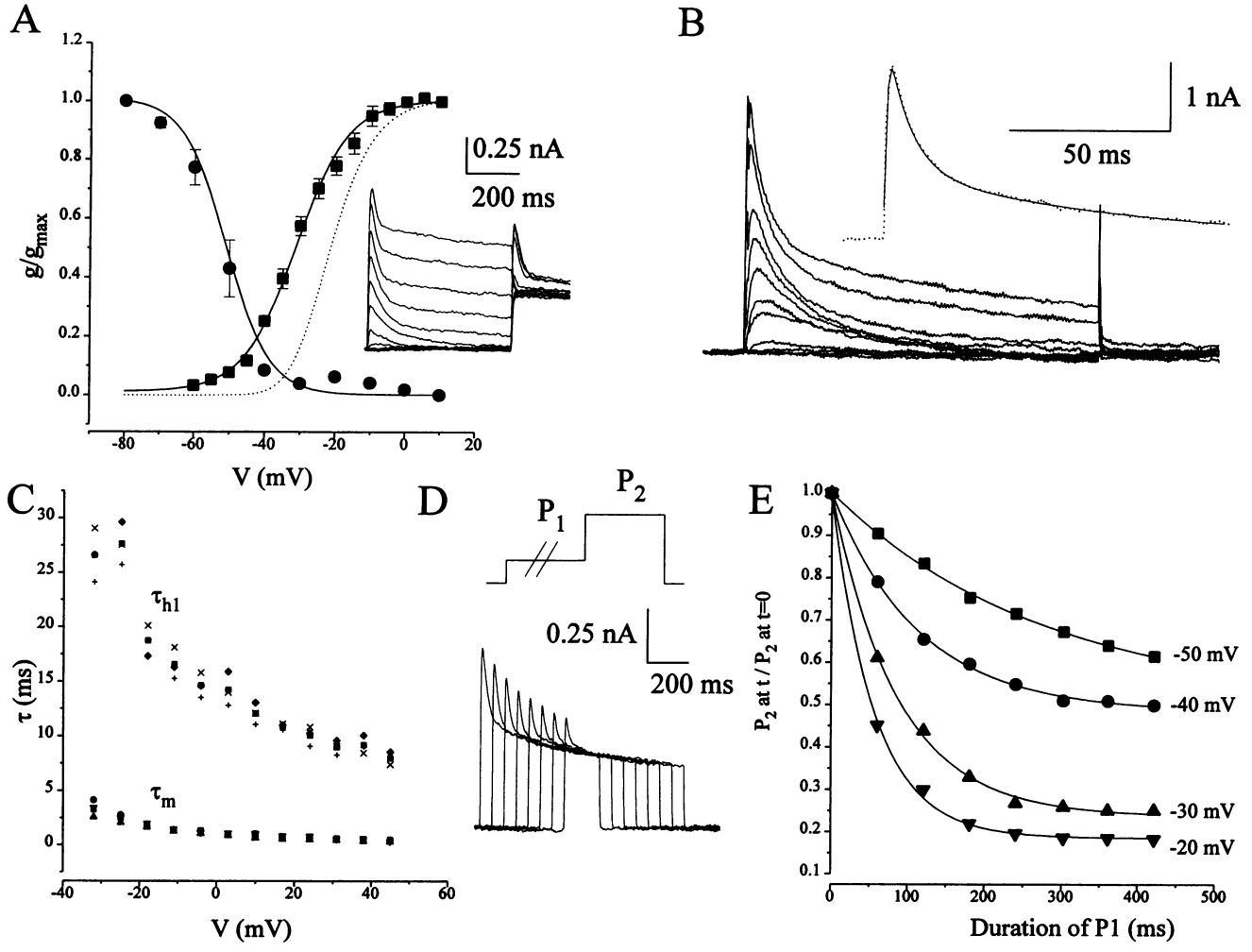

FIGURE 4 Voltage and time dependence of I_A. *A*, The steady-state activation (m_∞, ■) and inactivation (h_∞, ●) curves of I_A current were fitted with a Boltzmann function (*solid curves*; see Methods). The conductance of I_A was calculated with E_{rev} of −72 mV. The half-activation voltage ($V_{1/2}$) was −31 ± 1 mV, and the slope factor for the activation curve was 7.9 ± 0.4 mV (n = 9). The steady-state inactivation curve had a $V_{1/2}$ of −51 ± 0.8 mV and a slope factor of 6 ± 0.3 mV (n = 7). The inset shows examples of current traces elicited to generate the inactivation curve. The cell was held at −80 mV and stepped to conditioning potentials varying from −70 to 30 mV for 550 ms, followed by a test potential of 0 mV. The current was normalized against the noninactivating component evoked by the test potential. The dotted curve represents m^4_∞ obtained by direct calculation from the fitted m_∞ function. A small window conductance occurred from −50 to −30 mV, with a peak at −42 mV. *B*, 4-AP-sensitive current was obtained from the subtraction of current traces generated from a holding potential of −80 mV before and after application of 5 mM 4-AP. The current reveals an early transient followed by rapid inactivation. Equation 4 was used to fit the I_A records where m^4_∞ function and two time constants of inactivation yielded the best fit. Shown in the inset is an example of a current record (*dotted curve*) and the fit to the current trace (*solid curve*). *C*, Scatter plots of the time constants of activation (τ_m) and the fast component of inactivation (τ_{h1}) of I_A at various potentials. *D*, Time-dependent inactivation of I_A. Cells were held at −80 mV and stepped to conditioning prepulses (P_1) at various time intervals (t) before a test pulse to 10 mV (P_2) was delivered to determine the time-dependent inactivation of I_A at various membrane potentials. The lower panel shows a family of characteristic current traces obtained from P_2 elicited with a P_1 of −50 mV. *E*, The peak currents elicited with the test pulse (P_2) at various durations of P_1 (t) normalized to the peak current in the absence of the prepulse (P_2 at t = 0) and plotted against the duration of the prepulse (P_1). The time constants of the inactivation at −50 (■), −40 (●), −30 (▲), and −20 (▼) mV were 270 ± 46, 114 ± 23, 87 ± 18, and 56 ± 14 ms, respectively (n = 7).

of a double-pulse protocol. Cells were held at −80 mV and then stepped to various depolarizing prepulses for periods between 0 and 420 ms in 50-ms increments before a constant test pulse to 10 mV was applied. The peak transient outward current decreased as the duration of the prepulse was increased (Fig. 4 *D* and *E*). In the plot shown in Fig. 4 *E* the prepulse potential determined the time-dependent inactivation of the current. The average time constants of the time-dependent inactivation at −50, −40, −30, and −20 mV prepulses were 270, 114, 87, and 56 ms, respectively (n = 7).

Properties of the TEA-sensitive K^+ current

To isolate the TEA-sensitive current from other outward currents, hair cells were bathed in solution containing 0 Ca^{2+} (to suppress the Ca^{2+}-activated K^+ current) and 5

mM 4-AP (to block I_A). Alternatively, in a 0-Ca^{2+} recording solution, cells were held at −30 mV to avoid I_A contamination of the current. The outward current traces thus obtained from depolarizing pulses exhibited outward rectification and showed a decline in magnitude during prolonged pulses, especially at more positive potentials (Fig. 5 *A*). As a result of properties shared by the Hodgkin–Huxley delayed rectifier current and the TEA sensitivity, the current will be called $I_{K,V}$. $I_{K,V}$ in hair cells was insensitive to 4-AP and the effect of 4-AP was nonspecific and irreversible (Fig. 5 *B*). The voltage-dependent activation of the current can be described by a Boltzmann distribution with a half-activation voltage of 8.2 ± 0.7 mV and a slope factor of 9.6 ± 1.1 mV (n = 7; Fig. 5 *C*). Illustrated in Fig. 5 *D* are I_{KV} traces that were fitted with a modified version of Eq. 4. m_∞^3 was the best fit for I_{KV}.

Ca^{2+}-activated K^+ current

Voltage-clamp experiments conducted in the presence of external Ca^{2+}, TEA, and 4-AP revealed the existence of an outward current activated by depolarizing steps. The Ca^{2+}-activated K^+ current ($I_{K,Ca}$) was evoked at potentials positive to −40 mV. Fig. 6 *A* was obtained from a hair cell in the presence of 5 mM external Ca^{2+}. The outward current had a slow onset and deactivated with a time course of 5 to 25 ms at the end of the step potential. Shown in Fig. 6 *B* is

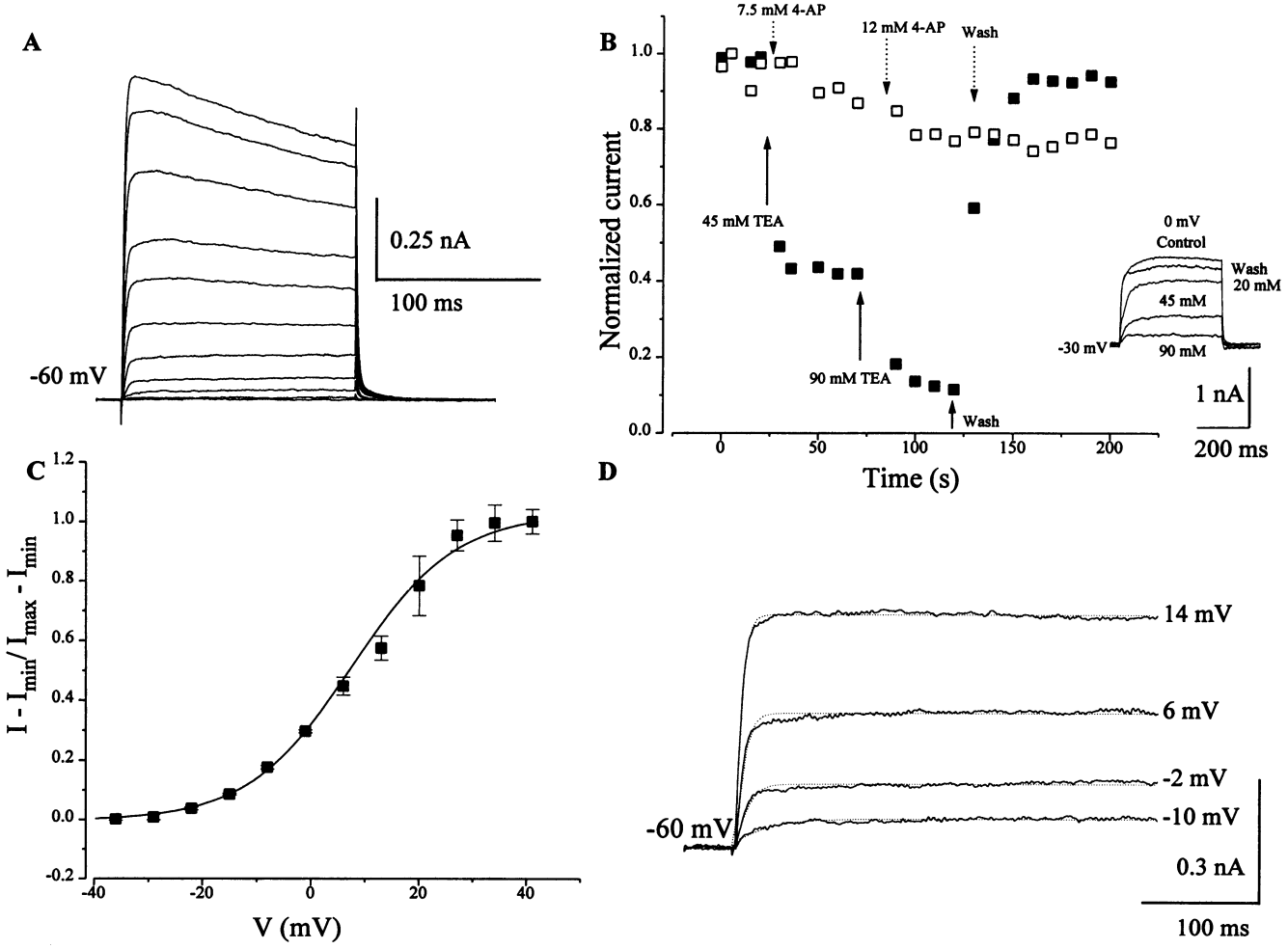

FIGURE 5 Delayed rectifier K^+ current ($I_{K,V}$). *A*, Current traces evoked from a holding potential of −60 mV by step depolarization from −40 to +60 mV in 9-mV increments. The experiment was conducted in a Ca^{2+}-free solution containing 5 mM 4-AP. Within the relevant physiological membrane potentials (−50 to 15 mV) the current showed little inactivation. However, at step potentials of >30 mV the evoked-current traces showed slow inactivation. *B*, Blocking of $I_{K,V}$ by TEA and 4-AP. The filled squares show the time course of the TEA effect on normalized $I_{K,V}$. Blockade of $I_{K,V}$ by TEA was concentration dependent, and the current recovered after washout. Shown in the inset are some of the traces used to generate the plot. The effects of 4-AP on $I_{K,V}$ are also shown (□). Note that 5 mM 4-AP was already present in the bath at the beginning of the experiment (t = 0). High concentrations of 4-AP (12 mM) appeared to reduce $I_{K,V}$ in an irreversible manner. *C*, Steady-state activation of $I_{K,V}$. The normalized current was plotted against the membrane voltage (V) and fitted with a Boltzmann function with a $V_{1/2}$ of 7.5 ± 0.7 mV and a slope factor of 9.6 ± 0.3 mV (n = 8). I_{min} represents the minimum current evoked, and I_{max} is the maximum current elicited. *D*, Fits (*dotted curves*) of Eq. 4 to $I_{K,V}$ records (*solid curves*) from one cell are illustrated. The inactivation component of the equation was removed, and $m^3{}_\infty$ represents the best fit to $I_{K,V}$.

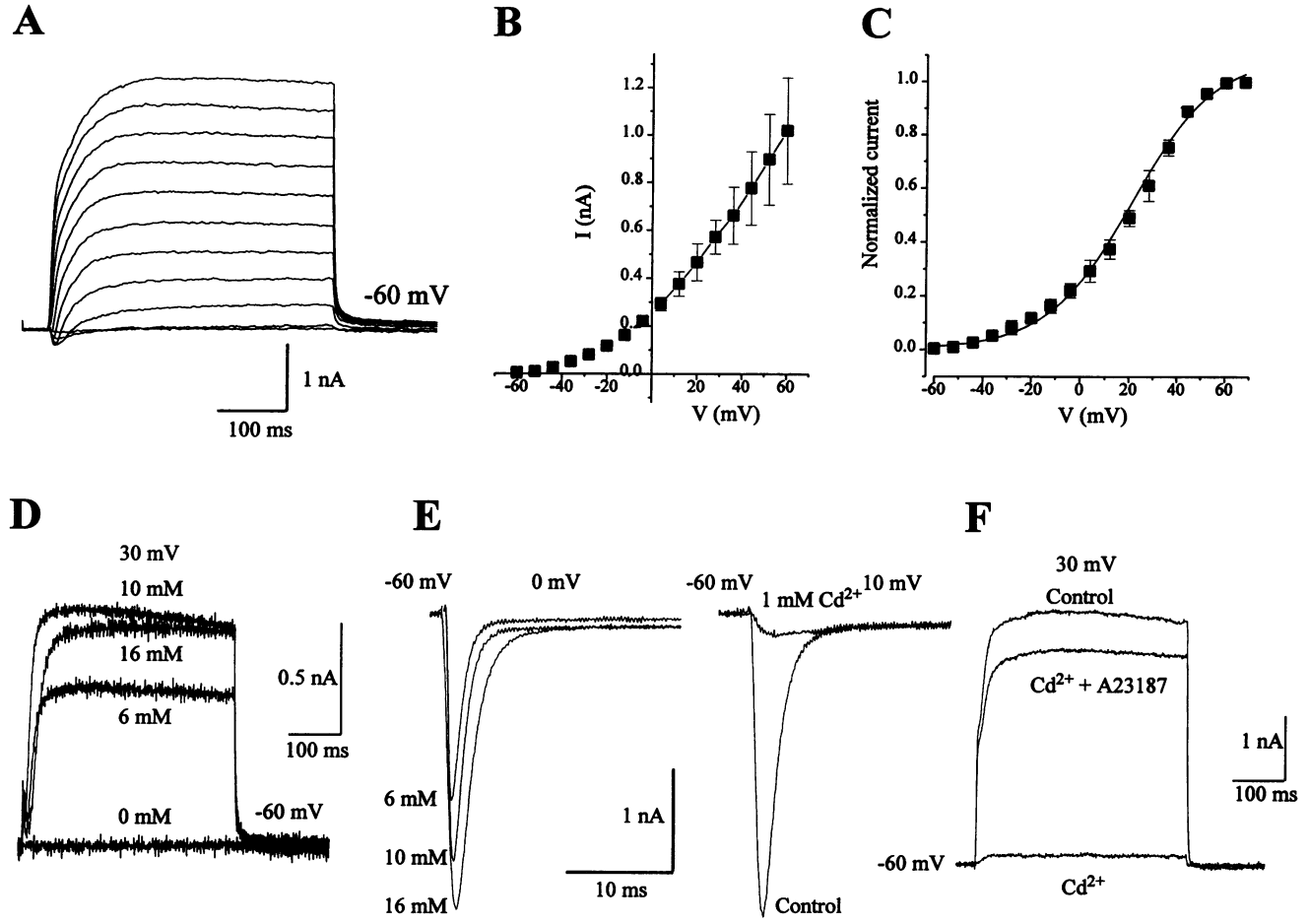

FIGURE 6 Ca^{2+}-activated K^+ current. *A*, A family of current traces evoked from step potentials of −60 mV to 60 mV in 8-mV increments. *B*, Current–voltage relation from seven cells. The current was measured from the steady-state level between 300 to 400 ms. Ca^{2+} currents in the hair cells decayed with a time course of less than 100 ms (*E*); therefore at 300 ms the contamination of $I_{K,Ca}$ by the Ca^{2+} current is expected to be minimal. *C*, The steady-state activation of $I_{K,Ca}$ was generated from the tail currents at different membrane voltages. The normalization procedure was similar to that for Fig. 5 *C*. The half-activation voltage ($V_{1/2}$) was 24 mV, and the slope factor was 16.6 mV. *D*, Traces of $I_{K,Ca}$ showing the Ca^{2+} dependence and the saturation concentration of Ca^{2+} (10 mM). The current traces were elicited from −60 mV to 30 mV. The concentration of bath Ca^{2+} is indicated beside each trace. *E*, Ca^{2+} currents, on the other hand, continued to increase at external Ca^{2+} higher than 10 mM. The current traces were elicited from −60 mV to 0 mV. Ca^{2+} currents were recorded with an external solution containing (in mM) 6–16 Ca^{2+}, 400 choline, 10 HEPES, 5 4-AP, 90 TEA, 10 Cs^+, 30–50 Mg^{2+}, and 10 glucose at pH 7.6 (CsOH). The pipette solution contained (in mM) 400 Cs^+, 3 Mg^{2+}, 5 ATP, 1 GTP, and 10 glutathione at pH 7.4 (TEAOH). The right-hand panel of *E* illustrates that Ca^{2+} currents in hair cells are blocked by Cd^{2+} (1 mM). Traces were evoked from −60 mV to 10 mV. *F*, $I_{K,Ca}$ was elicited from a holding potential of −60 mV by use of a test potential of 30 mV (control). 1 mM Cd^{2+} also blocked the $I_{K,Ca}$; however, in the presence of the Ca^{2+} ionophore, A23187 (2 μM), $I_{K,Ca}$ was resistant to block by Cd^{2+}. The effects of Ca^{2+} ionophore were seen 15–20 min after application.

a typical example of a current–voltage relationship of $I_{K,Ca}$. The activation curve was steepest between −15 and 30 mV, and the midpoint of activation ($V_{1/2}$) was at 24 mV (Fig. 6 *C*). Saturation of the Ca^{2+} dependence of the current was observed at 10 mM external Ca^{2+} concentration (Fig. 6 *D*). In contrast, the magnitude of the voltage-dependent Ca^{2+} current (I_{Ca}) increased as the external Ca^{2+} was raised above 10 mM (Fig. 6 *E*, *left panel*). I_{Ca} was blocked by 1 mM Cd^{2+} (Fig. 6 *E*, *right panel*). The same concentration of Cd^{2+} also blocked $I_{K,Ca}$ (Fig. 6 *F*). To test whether the effect of Cd^{2+} on $I_{K,Ca}$ was a direct consequence of blocking of $I_{K,Ca}$ channels or an indirect result of blocking of voltage-gated Ca^{2+} current, cells were superfused with a solution containing 1 mM Cd^{2+} or 1 mM Cd^{2+} and 2 μM A23187 (Ca^{2+} ionophore; this should promote Ca^{2+} influx, which is independent of influx through voltage-gated Ca^{2+} channels). In a group of three cells, currents elicited from −60 mV to 30 mV were 0.71 ± 0.16 nA in the control condition, 0.15 ± 0.06 nA in the presence of Cd^{2+}, and 0.56 ± 0.17 nA in the presence of Cd^{2+} and A23187. An example of typical results from such experiments is shown in Fig. 6 *F*. Cd^{2+} blocked the voltage-gated Ca^{2+} current and $I_{K,Ca}$, but, in the presence of A23187, which should permit Ca^{2+} influx that is independent of voltage-gated channels (Yamoah and Crow, 1995), Cd^{2+} did not produce any marked effect on $I_{K,Ca}$. Thus, the effect of Cd^{2+} on $I_{K,Ca}$ can be attributed to blocking of the voltage-gated Ca^{2+} current.

DISCUSSION

Previous studies of associative conditioning in *Hermissenda* showed that temporal convergence of excitation of the presynaptic hair cells and postsynaptic photoreceptors is necessary for enhanced type-B photoreceptor excitability, which underlies the induction of associative memory (Matzel and Alkon, 1991; Alkon et al., 1993). The electrical properties of hair cells and the underlying associative memory mechanisms have not been studied extensively. What little is known is that releases of GABA from the hair cells and serotonin, perhaps through interneurons, are presynaptic components for the mechanisms of plasticity in the vestibulo-visual system (Farley and Wu, 1987; Crow, 1988; Alkon et al., 1993; Talk and Matzel, 1996). Because the release of GABA and serotonin depends on electrical properties of the hair cells, the aim of the present study was to characterize the properties of voltage-activated K^+ currents that are partly responsible for membrane electrical properties. The data presented in this study indicate that presynaptic hair cells of *Hermissenda* express three major outward K^+ currents: a transient I_A-like current, a TEA-sensitive outward rectifying current ($I_{K,V}$), and a TEA- and 4AP-insensitive Ca^{2+}-activated K^+ current ($I_{K,Ca}$).

Voltage clamp and isolation of K^+ currents in hair cells

Hair cells in *Hermissenda* are electrically coupled at the axonal region, several micrometers away from the soma (Detwiler and Alkon, 1973; Grossman et al., 1979). Previous studies showed that partial axotomy of the static nerve in a semi-intact nervous system is sufficient to remove the electrical synapses between the hair cells (Detwiler and Alkon, 1973). Here, complete axotomy of the static nerve was made, and the capsule around the statocyst was carefully dissected to expose the hair cells for voltage-clamp studies. Current records from isolated cells and from those partially attached to the isolated statocyst were similar. The results show that the outward currents recorded in the hair cells are conducted by K^+ ions. Evidence for this is as follows: 1) By the method of exclusion, the permeant ions that could account for the outward currents recorded were Cl^- and K^+. Because the current magnitude was unaffected by alteration of either the external or the pipette [Cl^-] and no shift in the reversal potential of the current was detected as the external [Cl^-] was changed, Cl^- conductance was ruled out. 2) The reversal potential shifted in the direction expected for a K^+ conductance. 3) The pharmacology of the different components of the outward current is consistent with the conclusion that the currents were conducted by K^+.

Transient outward K^+ current (I_A)

Since I_A was first described in *Onchidium* and *Anisodoris* neurons (Hagiwara et al., 1961; Connor and Stevens, 1971), it has become increasingly evident that the current is a common feature of excitable cells (Ruby, 1988; Belluzzi and Sacchi, 1991; Hille, 1992). The functions of I_A differ, however, from cell to cell. Whereas it has been shown to be responsible for the shape and the frequency of firing of action potentials (Connor and Stevens, 1971; Cassel et al., 1986) and to modulate synaptic potentials in snail neurons and sympathetic ganglion cells (Daut, 1973; Cassel and McLachlan, 1986), in *Hermissenda* photoreceptors modulation of I_A has been correlated to plasticity following classical conditioning (Alkon, 1984; Nelson et al., 1990; Farley and Auerbach, 1986). An I_A-like current controls the dampened membrane-voltage oscillation in hair cells in goldfish sacculus (Sugihara and Furukawa, 1995). Despite the functional differences expressed by I_A in different cells, there are several features shared by the current. These include voltage-dependent activation and inactivation, substantial removal from inactivation after small membrane hyperpolarization, sensitivity to 4-AP, and, in some cases, complete steady-state inactivation at potentials close to the resting potential. Although I_A in some systems is sensitive to TEA (Kros and Crawford, 1990), such was not the case in *Hermissenda* hair cells. The fast activation time constant (<10 ms) is similar to that reported for I_A in goldfish hair cells (Sugihara and Furukawa, 1995), but I_A in *Hermissenda* hair cells has inactivation time constants that are much faster than those in goldfish hair cells (>600 ms) (Sugihara and Furukawa, 1995). Differences in the kinetics of I_A subtypes have been described in molluscan neurons, and the evidence suggests that I_A is expressed in a cell-specific fashion (Serrano and Getting, 1989; Premach et al., 1989; Acousta-Urquidi and Crow, 1995). Therefore, I_A subtypes consist of a heterogeneous family of currents with a broad range of genetically specified kinetics (Miller, 1990). The A-current recorded from hair cells in *Hermissenda* is slightly activated at the resting potential (-50 to -60 mV), and the presence of a window current (-50 to -30 mV) close to the resting potential suggests that the current may serve to maintain the resting potential close to the E_{rev} of K^+. Window currents of I_A close to the resting potential have been demonstrated in cerebellar granule cells and lactotroph cells (Bardoni and Belluzzi, 1993; Lledo et al., 1990). This feature of the transient outward current makes it a likely candidate for the modulation of hair-cell excitability and action potential firing. The sensitivity of the activation of I_A to voltage shows that I_A increases *e*-fold every 3.5 mV. This sensitivity of I_A to voltage is comparable with that of the A-current recorded in goldfish hair cells (Sugihara and Furukawa, 1995) and that of the Ca^{2+}-activated K^+ currents in frog sacculus (Hudspeth and Lewis, 1988), where these K^+ conductances are known to regulate dampened oscillation of membrane potential.

TEA-sensitive K^+ current

The TEA-sensitive K^+ current in *Hermissenda* hair cells is similar to the delayed rectifier K^+ current ($I_{K,V}$) described

in the squid giant axon (Hodgkin and Huxley, 1952). The activation of the current is voltage dependent (increase of *e*-fold/9 mV), and the current exhibits slow inactivation. Like $I_{K,V}$ in other systems (Ruby, 1988), the current was blocked by TEA. However, unlike $I_{K,V}$ in the squid giant axon and in the sensory neurons of *Aplysia* (Ruby, 1988; Baxter and Byrne, 1989), $I_{K,V}$ in hair cells of *Hermissenda* shows little sensitivity to 4-AP. Whereas 2 mM 4-AP was sufficient to block $I_{K,V}$ in *Aplysia* pleural sensory neurons (Baxter and Byrne, 1989), more than 12 mM was needed to block 20% of the current in hair cells. It appears that the blocking effect of 4-AP differs from tissue to tissue and varies among species (Miller, 1990). Moreover, the mechanisms of blockade by 4-AP on K^+ channels differ in different systems: 4-AP blocks the outward K^+ current in B lymphocytes in a use-dependent fashion, indicating an open channel block (Choquet and Korn, 1992), whereas the transient outward K^+ current in ventricular myocytes is blocked by 4-AP in the closed state (Campbell et al., 1993). Variations in the blocking mechanism of 4-AP on outward K^+ currents may reflect the fact that delayed rectifier K^+ channels comprise heterogeneous groups of channels (Miller, 1990). Because $I_{K,V}$ in *Hermissenda* hair cells activates at voltages positive to -25 mV that are positive to the hair cells' action potential threshold, this current is likely to play a role in the repolarization phase of the action potential rather than modulating the frequency of firing or suppressing synaptic inputs (Cassell et al., 1986).

Ca^{2+}-activated K^+ current

Application of 5 mM 4-AP and 90 mM TEA suppressed outward currents elicited from −80 mV to depolarizing voltages in the Ca^{2+}-free solution. However, a large noninactivating outward current can be evoked on application of Ca^{2+}. A Ca^{2+}-dependent Cl^- current could be ruled out because changes in the external [Cl^-] did not shift the apparent reversal potential of the current (data not shown). In addition, the current reversed close to the K^+ equilibrium potential, suggesting that K^+ ions were the charge carriers. The dependence of the current on Ca^{2+} was further suggested by experiments that showed that the outward current could be blocked by Cd^{2+}, which blocked I_{Ca}. However, Cd^{2+} did not directly block the Ca^{2+}-activated K^+ channel because application of 2 μM A23187 restored the outward current, even in the presence of Cd^{2+}. This current is insensitive to TEA, unlike $I_{K,Ca}$ or maxi channels in vertebrates (Ruby, 1988; Hille, 1992) but similar to the slow apamin-sensitive currents in neuroblastoma cells (Hugues et al., 1982). According to the nomenclature of $I_{K,Ca}$ (Ruby, 1988; Hille, 1992) the current described from *Hermissenda* hair cells can be considered a Ca^{2+}-activated afterhyperpolarization current (I_{AHP}). However, $I_{K,Ca}$ in hair cells was strongly voltage dependent, whereas I_{AHP} has little or no voltage dependence (Hille, 1992). Hair cells have a characteristic depolarization plateau phase after mechanical stimulation (Talk and Matzel, 1996) followed by a prolonged afterhyperpolarization. Potentially, $I_{K,Ca}$ can be responsible for the afterhyperpolarization. Ca^{2+} influx through voltage-gated Ca^{2+} channels during the plateau phase will activate $I_{K,Ca}$, which in turn will induce a sustained repolarization of the membrane potential. Furthermore, in vertebrate hair cells, in which the resonant frequency has been studied in detail, a slow voltage-dependent Ca^{2+}-activated K^+ current is responsible for this property (Art et al., 1993; Hudspeth and Lewis, 1988). Although the resonance frequency of *Hermissenda* hair cells has not been studied, it is speculated that $I_{K,Ca}$ may play a role in the frequency of membrane potential oscillations.

A prominent feature of classical conditioning in the *Hermissenda* nervous system is the significant increase in post-pairing (paired stimulation of hair cells and photoreceptors) synaptic potential frequency in the B cells (Farley and Alkon, 1987). The changes in synaptic properties that are detected in the B cells may result from changes in presynaptic release of neurotransmitters in conjunction with the changes in the intrinsic properties of the B cells. A current such as I_A in hair cells could conceivably be altered to produce conditioning-specific responses.

I thank Dr. T. Crow for providing the laboratory space and funds for this research and Dr. J. Byrne for the use of the osmometer in his laboratory. I am also grateful to Ms Vilma Saddiqui for her help in dissection and isolation of the statocyst organ. Dr. N. Chiamvimonvat, Dr. H. Bradley Nuss, and Dr. P. G. Gillespie provided helpful discussions and comments.

REFERENCES

Abrams, T. W., and E. R. Kandel. 1988. Is contiguity detection in classical conditioning a system or a cellular property? Learning in *Aplysia* suggests a possible molecular site. *Trends Neurosci.* 11:128–135.

Acosta-Urquidi, J., and T. Crow. 1995. Characterization of voltage-activated currents in *Hermissenda* type B-photoreceptors. *J. Neurosci.* 15:319–332.

Alkon, D. L. 1975. Responses of hair cells to statocyst rotation. *J. Gen. Physiol.* 66:507–530.

Alkon, D. L. 1984. Calcium-mediated reduction of ionic currents: a biophysical memory trace. *Science.* 226:1037–1045.

Alkon, D. L., M. J. Anderson, A. Kuzirian, D. F. Rogers, D. M. Fass, C. Collin, T. J. Nelson, I. M. Kapetanovic, and L. D. Matzel. 1993. GABA-mediated synaptic interaction between the visual and vestibular pathways of *Hermissenda*. *J. Neurochem.* 61:556–566.

Alkon, D. L., and A. Bak. 1973. Hair cell generator potentials. *J. Gen. Physiol.* 61:619–637.

Alkon, D. L., J-V. Sanchez-Andres, E. Ito, K. Oka, T. Yoshioka, and C. Collin. 1992. Long-term transformation of an inhibitory into an excitatory GABAergic synaptic response. *Proc. Natl Acad. Sci. USA.* 89: 11,862–11,866.

Art, J. J., R. Fettiplace, and Y.-C. Wu. 1993. The effects of low calcium on the voltage-dependent conductances involved in tuning of turtle hair cells. *J. Physiol.* 470:109–126.

Bardoni, R., and O. Belluzzi. 1993. Kinetic study and numerical reconstruction of A-type current in granule cells of rat cerebellar slices. *J. Neurophysiol.* 69:2222–2231.

Baxter, D. A., and J. H. Byrne. 1989. Serotonergic modulation of two potassium currents in the pleural sensory neuron of *Aplysia*. *J. Neurophysiol.* 62:665–679.

Bekkers, J. M., and C. F. Stevens. 1990. Presynaptic mechanisms for long-term potentiation in the hippocampus. *Nature (London).* 361: 31–39.

Belluzzi, O., and O. Sacchi. 1990. The calcium-dependent potassium conductance in rat sympathetic neurons. *J. Physiol.* 422:561–583.

Belluzzi, O., and O. Sacchi. 1991. A five-conductance model of the action potential in the rat sympathetic neurone. *Prog. Biophys. Molec. Biol.* 55:1–30.

Campbell, D. L., Y. Qu, R. L. Rasmusson, and H. C. Stauss. 1993. The calcium-independent transient outward potassium current in isolated ferret right ventricular myocytes. II. Closed state reverse use-dependent block by 4-aminopyridine. *J. Gen. Physiol.* 101:603–623.

Cassel, J. F., A. L. Clark, and E. M. McLachlan. 1986. Characteristics of phasic and tonic sympathetic ganglion cells of the guinea-pig. *J. Physiol.* 372:457–483.

Cassel, J. F., and E. M. McLachlan. 1986. The effects of a transient outward current on synaptic potentials in sympathetic ganglion cells of the guinea pig. *J. Physiol.* 374:273–288.

Chavez-Noriega, L. E., and C. F. Stevens. 1994. Increased transmitter release at excitatory synapse produced by direct activation of adenylate cyclase in rat hippocampal slices. *J. Neurosci.* 14:310–317.

Choquet, D., and H. Korn. 1992. Mechanisms of 4-aminopyridine action on voltage-gated potassium channels in lymphocytes. *J. Gen Physiol.* 99:217–240.

Connor, J. A., and C. F. Stevens. 1971. Voltage clamp studies of a transient outward membrane current in gastropod neural somata. *J. Physiol.* 213:21–30.

Crow, T. 1988. Cellular and molecular analysis of associative learning and memory in *Hermissenda*. *Trends Neurosci.* 11:136–142.

Daut, J. 1973. Modulation of the excitatory synaptic response by fast transient K^+ current in snail neurones. *Nature (London).* 246:193–196.

DeFelice, L. J., and D. L. Alkon. 1977. Voltage noise from hair cells during mechanical stimulation. *Nature (London).* 269:613–615.

Detwiller, P. B., and D. L. Alkon. 1973. Hair cell interactions in the statocyst of *Hermissenda*. *J. Gen. Physiol.* 62:618–642.

Farley, J., and D. L. Alkon. 1987. In vitro associative conditioning of *Hermissenda*: cumulative depolarization of type B photoreceptors and short-term associative behavioral changes. *J. Neurophysiol.* 57: 1637–1668.

Farley, J., and S. Auerbach. 1986. Protein kinase C activation induces conductance changes in *Hermissenda* photoreceptors like those seen in associative learning. *Nature (London).* 319:220–223.

Farley, J., and R. Wu. 1989. Serotonin-modulation of *Hermissenda* B photoreceptor ionic currents. *Brain Res Bull.* 22:335–351.

Grossman, Y., D. L. Alkon, and E. Heldman. 1979. A common origin of voltage noise and generator potential in statocyst hair cells. *J. Gen. Physiol.* 73:23–48.

Hagiwara, S., K. Kusano, and N. Saito. 1961. Membrane changes of *Onchidium* nerve cell in potassium-rich media. *J. Physiol.* 155:470–489.

Hamill, O. P., A. Marty, E. Neher, B. Sakmann, and F. J. Sigworth. 1981. Improved patch-clamp techniques for high resolution current recording from cells and cell-free membrane patches. *Pfluegers Arch.* 391:85–100.

Hille, B. 1992. Ionic Channels of Excitable Membranes, 2nd ed. Sinauer Associates, Inc., Sunderland, MA.

Hodgkin, A. L., and A. F. Huxley. 1952. Currents carried by sodium and potassium ions through the membrane of giant axon of *Loligo*. *J. Physiol.* 116:449–472.

Hudspeth, A. J., and R. Jacobs. 1979. Stereocilia mediate transduction in vertebrate hair cells. *Proc. Natl. Acad. Sci. USA.* 76:1506–1509.

Hudspeth, A. J., and R. S. Lewis. 1988. A model for electrical resonance and frequency tuning in saccular hair cells of the bullfrog, *Rana catesbeiana*. *J. Physiol.* 400:275–297.

Hugues, M., G. Romey, D. Duval, J. Vincent, and P. Lazdunski. 1982. Apamin as a selective blocker of the calcium dependent potassium channel in neuroblastoma cells: voltage-clamp and biochemical characterization of the toxin receptor. *Proc. Natl. Acad. Sci. USA.* 79: 1308–1312.

Kros, C. J., and A. C. Crawford. 1990. Potassium currents in inner hair cells isolated from the guinea-pig cochlea. *J. Physiol.* 421:263–291.

Kuzirian, A. M., D. L. Alkon, and L. G. Harris. 1981. An infraciliary network in statocyst hair cells. *J. Neurocytol.* 10:497–514.

Land, P. W, and T. Crow. 1985. Serotonin immunoreactivity in the circumesophageal nervous system of *Hermissenda crassicornis*. *Neurosci Lett.* 62:199–205.

Lledo, P. M., P. Legendre, J. Zhang, J. M. Israel, and J. D. Vincent. 1990. Effects of dopamine on voltage-dependent potassium currents in identified rat lactotroph cells. *Neuroendocrinology.* 52:545–555.

Matzel, L. D., and D. L. Alkon. 1991. GABA-induced potentiation of neuronal excitability occurs during contiguous pairings with intracellular calcium elevation. *Brain Res.* 554:77–84.

Matzel, L. D., I. A. Muzzio, and R. F. Rogers. 1995. Diverse current and voltage responses to baclofen in an identified molluscan photoreceptor. *J. Neurophysiol.* 74:506–518.

Matzel, D. L., and R. F. Rogers. 1993. Postsynaptic calcium, but not cumulative depolarization is necessary for the induction of associative plasticity in *Hermissenda*. *J Neurosci.* 13:5029–5040.

Meech, R. W. 1974. The sensitivity of *Helix asperse* neurons to injected calcium ions. *J. Physiol.* 237:259–277.

Miller, C. 1990. Annus mirabilis of potassium channels. *Science.* 252: 1092–1096.

Nelson, T. J., C. Collin, and D. L. Alkon. 1990. Isolation of a G protein that is modified by learning and reduces potassium currents in *Hermissenda*. *Science.* 247:1479–1481.

Norris, C. H., A. J. Ricci, G. D. Housley, and P. S. Guth. 1992. The inactivating potassium currents of hair cells isolated from the crista ampullaris of the frog. *J. Neurophysiol.* 68:1642–1653.

Premach, B. A., S. Thompson, and J. Coombs-Hahn. 1989. Clustered distribution and variability in kinetics of transient K channels in molluscan neuron cell bodies. *J. Neurosci.* 9:4089–4099.

Rogers, R. F., D. M. Fass, and L. D. Matzel. 1994. Current, voltage and pharmacological substrates of a novel GABA receptor in the visual-vestibular system of *Hermissenda*. *Brain Res.* 50:93–106.

Ruby, B. 1988. Diversity and ubiquity of K channels. *Neuroscience.* 25:729–749.

Serrano, E. E., and P. A. Getting. 1989. Diversity of transient outward potassium current in somata of identified molluscan neurons. *J. Neurosci.* 9:4021–4032.

Stommel, E. W., R. E. Stephens, and D. L. Alkon. 1980. Motile statocyst cilia transmit rather than directly transduce mechanical stimuli. *J. Cell Biol.* 87:652–662.

Sugihara, I., and T. Furukawa. 1995. Potassium currents underlying the oscillatory response in hair cells of the goldfish sacculus. *J. Physiol.* 489:443–453.

Talk, A. C., and L. D. Matzel. 1996. Calcium influx and release from intracellular stores contribute differentially to activity-dependent plasticity in *Hermissenda* photoreceptors. *Neurobiol. Learning Memory.* In press.

Yamoah, E. N., and T. Crow. 1994. Two components of calcium currents in the soma of photoreceptors of *Hermissenda*. *J. Neurophysiol.* 72: 1327–1336.

Yamoah, E. N., and T. Crow. 1995. Evidence for a contribution of I_{Ca} to serotonergic modulation of $I_{K,Ca}$ in *Hermissenda* photoreceptors. *J. Neurophysiol.* 74:1349–1354.

Yamoah, E. N., and T. Crow. 1996. Protein kinase and G-protein regulation of Ca^{2+} currents in *Hermissenda* photoreceptors by 5-HT and GABA. *J. Neurosci.* 16:4799–4809.

Yamoah, E. N., and A. M. Kuzirian. 1994. Effects of GABA on outward currents in *Hermissenda* photoreceptors. *Biol. Bull.* 187:265–266.